Studies of physical model and 3D field data for evidence of fracture-induced azimuthal anisotropy

KHALED AL DULAIJAN*, GARY F MARGRAVE, AND JOE WONG

DECEMBER, 2014

Motivation

Information related to ***fracture intensity and orientation*** is vital for the development of unconventional reservoirs

Outline

- **Introduction**
- Part 1: **Physical modeling analysis**
  - **Stiffness coefficients calculation**
  - Traveltime analysis
  - S-wave splitting
- Part 2: **South Komie 3D data analysis**
  - **Post stack inversion**
  - **Post-stack attributes**
  - AVO analysis
- **Conclusions**

Seismic Anisotropy

CREWES

- **Why?**
  - **Exploration purposes: Improve seismic image (velocity/ focusing/ positioning)**
  - **Development purposes: Relate to fractures (fracture intensity/ fracture orientation)**
- **Classification (Exploration Geophysics):**
  - **1 axis of symmetry~ Transverse Isotropy: HTI, VTI, and TTI**
  - **3 orthogonal planes of symmetry~ Orthorhombic Isotropy**

Stiffness Coefficients Tensor

CREWES

Isotropy

2 parameters

$$C_{ij} = \begin{bmatrix} \lambda+2\mu & \lambda & \lambda & 0 & 0 & 0 \\ \lambda & \lambda+2\mu & \lambda & 0 & 0 & 0 \\ \lambda & \lambda & \lambda+2\mu & 0 & 0 & 0 \\ 0 & 0 & 0 & \mu & 0 & 0 \\ 0 & 0 & 0 & 0 & \mu & 0 \\ 0 & 0 & 0 & 0 & 0 & \mu \end{bmatrix}$$

λ & μ : Lame's constants

VTI

5 parameters

$$C_{ij} = \begin{bmatrix} C_{11} & C_{12} & C_{13} & 0 & 0 & 0 \\ C_{12} & C_{11} & C_{13} & 0 & 0 & 0 \\ C_{13} & C_{13} & C_{33} & 0 & 0 & 0 \\ 0 & 0 & 0 & C_{55} & 0 & 0 \\ 0 & 0 & 0 & 0 & C_{55} & 0 \\ 0 & 0 & 0 & 0 & 0 & C_{66} \end{bmatrix}$$

$C_{12} = C_{11} - 2C_{66}$

HTI

5 parameters

$$C_{ij} = \begin{bmatrix} C_{11} & C_{13} & C_{13} & 0 & 0 & 0 \\ C_{13} & C_{33} & C_{23} & 0 & 0 & 0 \\ C_{13} & C_{23} & C_{33} & 0 & 0 & 0 \\ 0 & 0 & 0 & C_{44} & 0 & 0 \\ 0 & 0 & 0 & 0 & C_{55} & 0 \\ 0 & 0 & 0 & 0 & 0 & C_{55} \end{bmatrix}$$

$C_{23} = C_{33} - 2C_{44}$

Orthorhombic

9 parameters

$$C_{ij} = \begin{bmatrix} C_{11} & C_{12} & C_{13} & 0 & 0 & 0 \\ C_{12} & C_{22} & C_{23} & 0 & 0 & 0 \\ C_{13} & C_{23} & C_{33} & 0 & 0 & 0 \\ 0 & 0 & 0 & C_{44} & 0 & 0 \\ 0 & 0 & 0 & 0 & C_{55} & 0 \\ 0 & 0 & 0 & 0 & 0 & C_{66} \end{bmatrix}$$

PART 1: PHYSICAL MODELING ANALYSIS

Physical Model

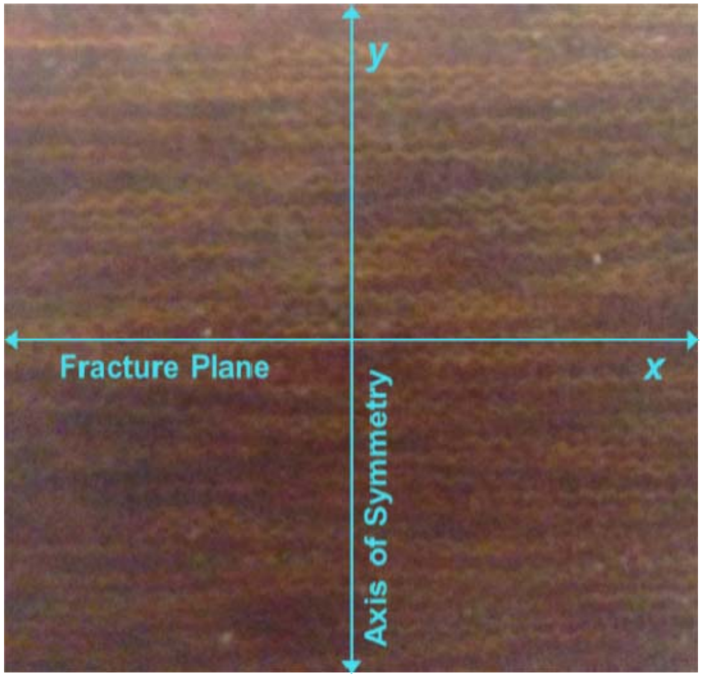

A zoomed-in photo of Phenolic

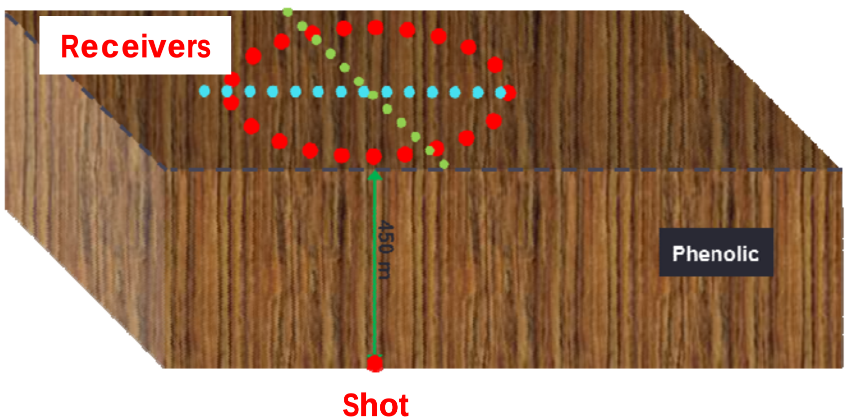

Acquisition layout:

One circular gather with 200 m radius

Two linear gathers with 0º and 90º azimuths

3-C receiver and 2-C horizontal source

Distribution of Receivers

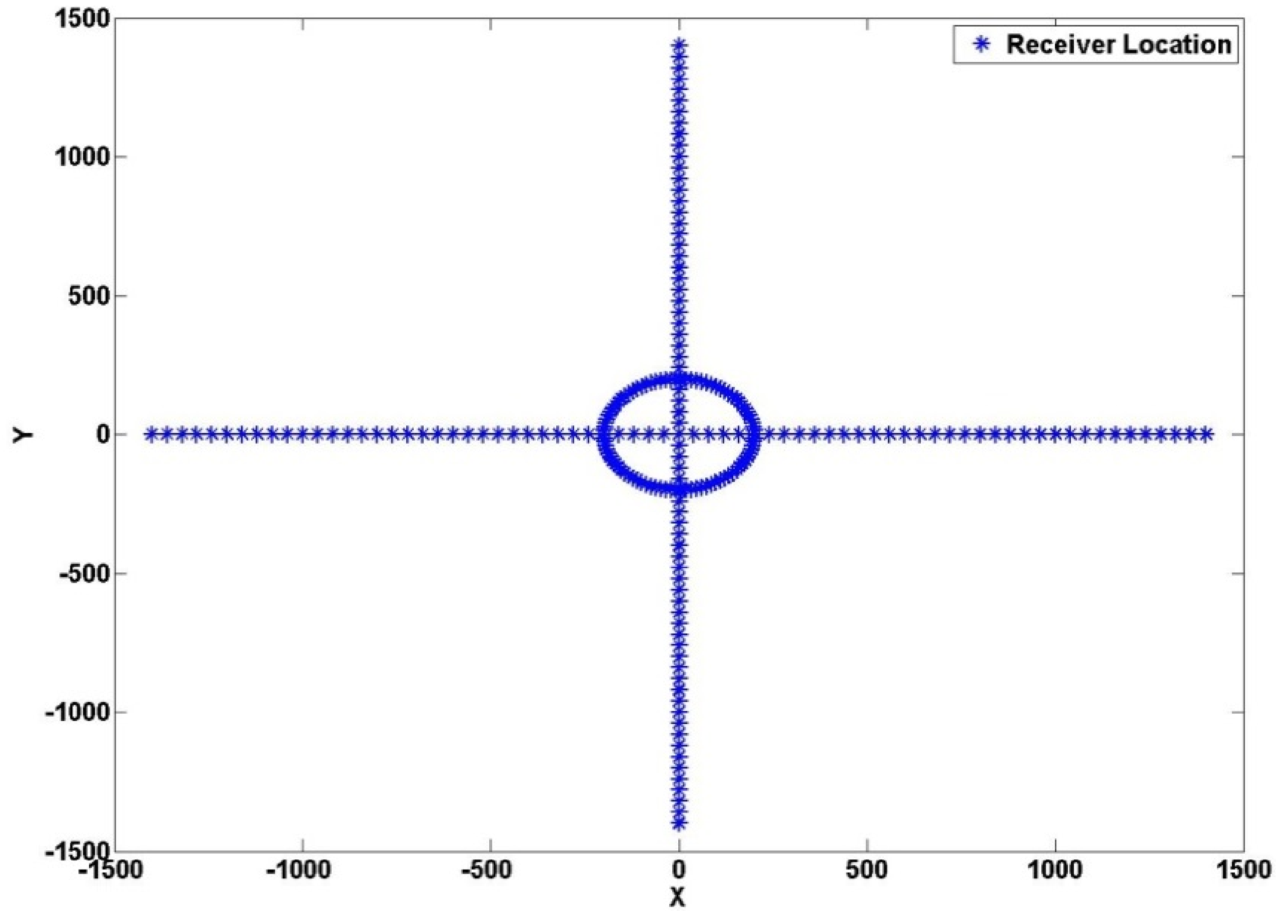

Azimuth & Incidence

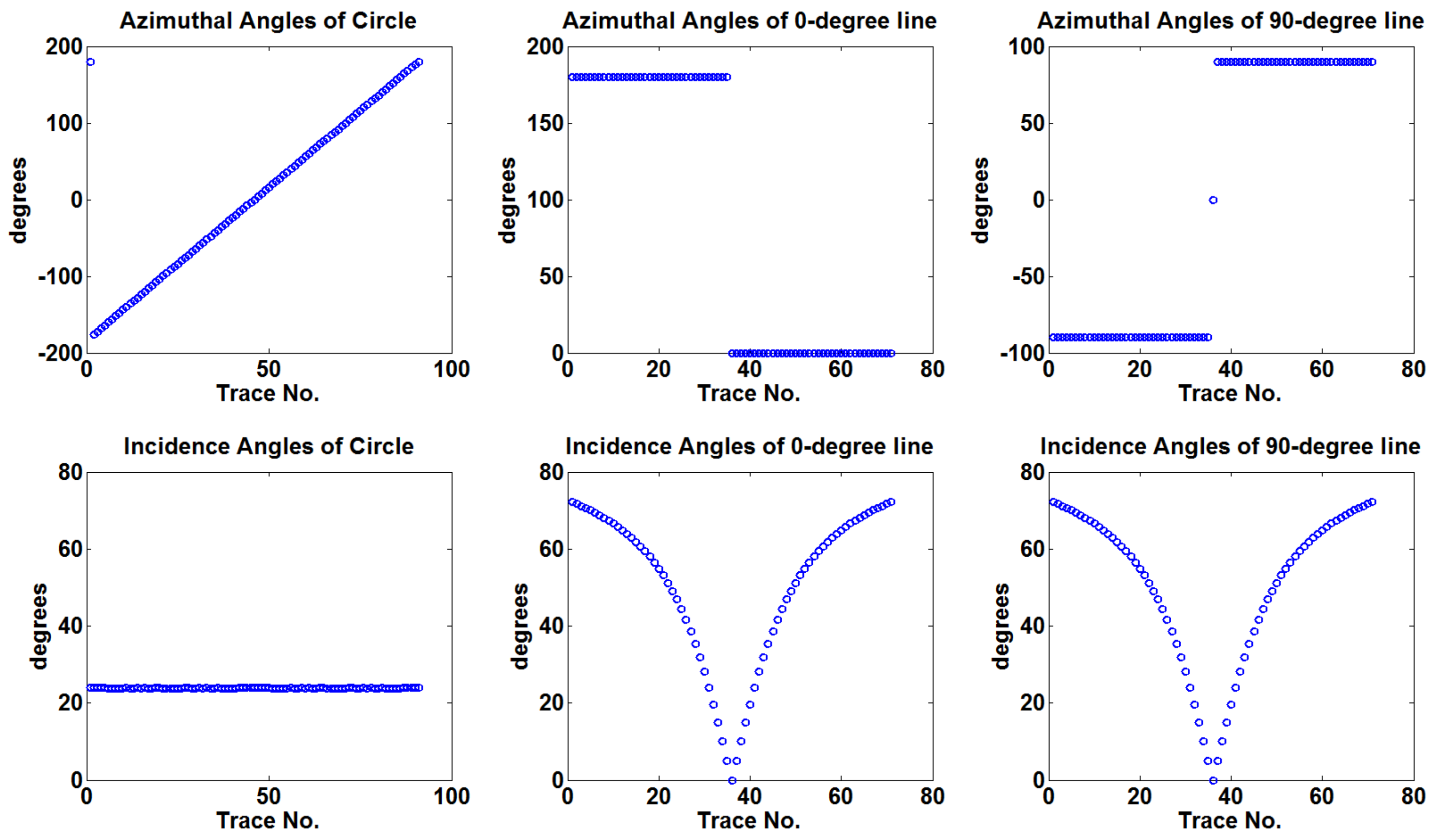

Gathers & First Breaks

200-m Circle

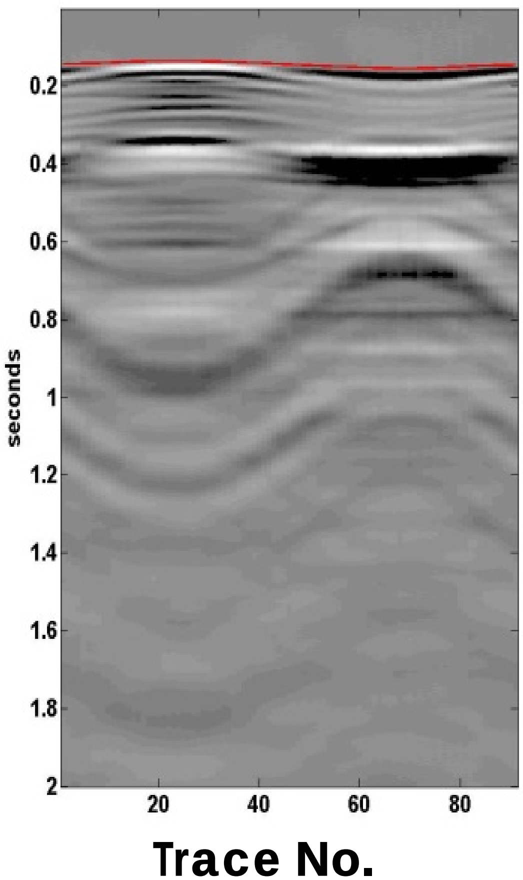

0º Azimuth

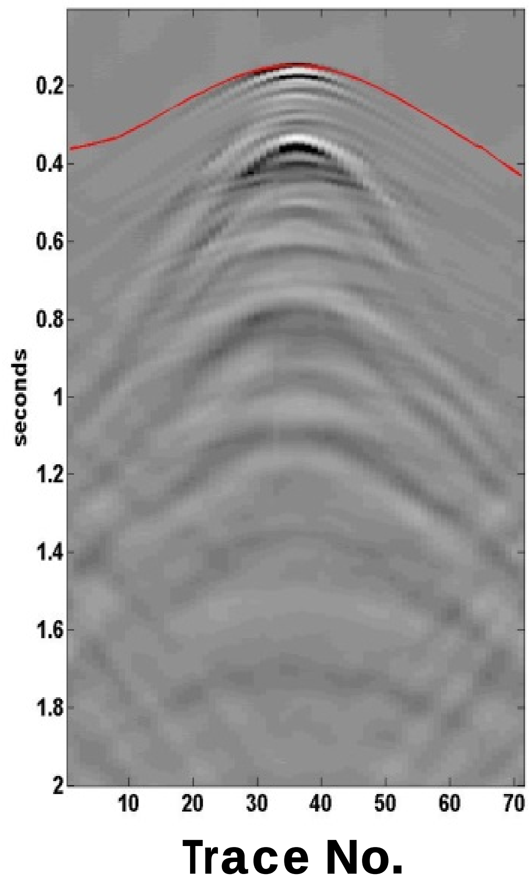

90º Azimuth

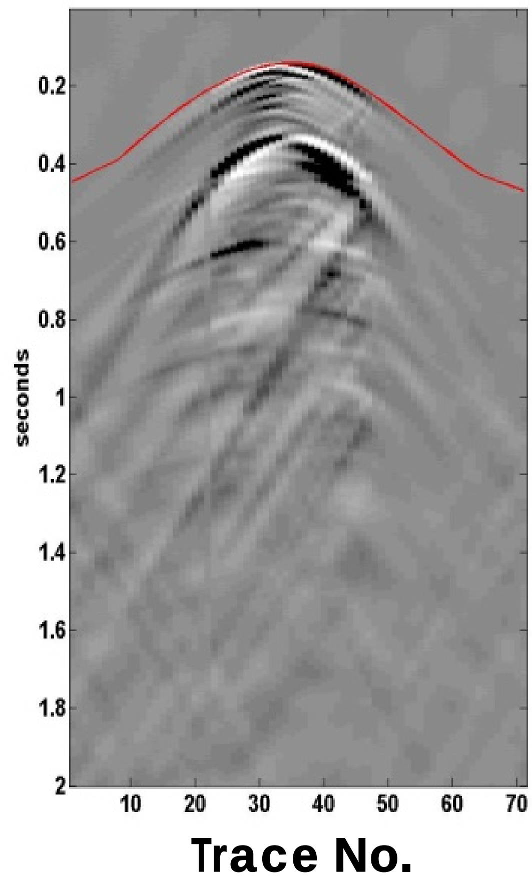

Density-normalized stiffness coefficients

- ***A_{ij}*** **is density normalized *C_{ij}***
- ***A_{ij}*** **is directly related to phase velocities**
- ***A_{ij}*** **can be measured from group velocities using Daley and Krebes (2006)**

$$\frac{1}{V^2(\vec{N})} \approx \frac{N_1^2}{A_{11}} + \frac{N_2^2}{A_{22}} + \frac{N_3^2}{A_{33}} - \frac{E_{23}N_2^2N_3^2}{A_{22}A_{33}} - \frac{E_{13}N_1^2N_3^2}{A_{11}A_{33}} - \frac{E_{12}N_1^2N_2^2}{A_{11}A_{22}}$$

$$\vec{N} = (N_1, N_2, N_3)$$

$$N_3 = \cos(\Phi)$$

$$N_1 = \sin(\Theta)\cos(\Phi)$$

$$N_2 = \sin(\Theta)\sin(\Phi)$$

$$E_{23} = 2(A_{23} + 2A_{44}) - (A_{22} + A_{33})$$

$$E_{13} = 2(A_{13} + 2A_{55}) - (A_{11} + A_{33})$$

$$E_{12} = 2(A_{12} + 2A_{66}) - (A_{11} + A_{22})$$

Density-normalized stiffness coefficients

$$\frac{1}{V^2(\vec{N})} = \frac{N_1^2}{A_{11}} + \frac{N_2^2}{A_{22}} + \frac{N_3^2}{A_{33}} - \frac{E_{23}N_2^2N_3^2}{A_{22}A_{33}} - \frac{E_{13}N_1^2N_3^2}{A_{11}A_{33}} - \frac{E_{12}N_1^2N_2^2}{A_{11}A_{22}}$$

$$d = Gm$$

$$\begin{bmatrix} \frac{1}{V_1^2} \\ \frac{1}{V_2^2} \\ \frac{1}{V_3^2} \\ \vdots \\ \frac{1}{V_n^2} \end{bmatrix} = \begin{bmatrix} N_{11}^2 & N_{21}^2 & N_{31}^2 & N_{21}^2N_{31}^2 & N_{11}^2N_{31}^2 & N_{11}^2N_{21}^2 \\ N_{12}^2 & N_{22}^2 & N_{32}^2 & N_{22}^2N_{32}^2 & N_{12}^2N_{32}^2 & N_{11}^2N_{22}^2 \\ N_{13}^2 & N_{23}^2 & N_{33}^2 & N_{23}^2N_{33}^2 & N_{13}^2N_{33}^2 & N_{13}^2N_{23}^2 \\ \vdots & & & & & \vdots \\ N_{1n}^2 & N_{2n}^2 & N_{3n}^2 & N_{2n}^2N_{3n}^2 & N_{1n}^2N_{3n}^2 & N_{1n}^2N_{2n}^2 \end{bmatrix} \begin{bmatrix} \frac{1}{A_{11}} \\ \frac{1}{A_{22}} \\ \frac{1}{A_{33}} \\ -\frac{E_{23}}{A_{22}A_{33}} \\ -\frac{E_{13}}{A_{11}A_{33}} \\ -\frac{E_{12}}{A_{11}A_{22}} \end{bmatrix}$$

Resolution Matrix

Resolution matrix all data

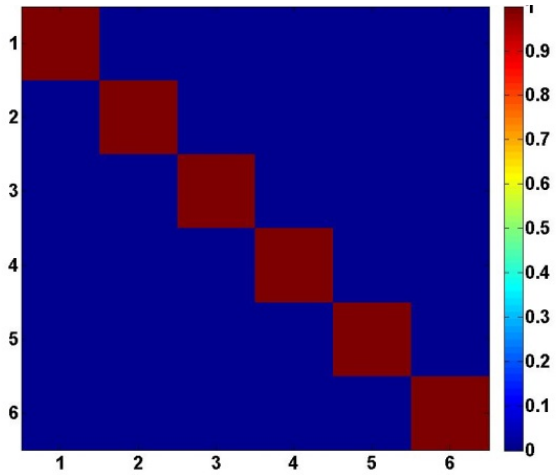

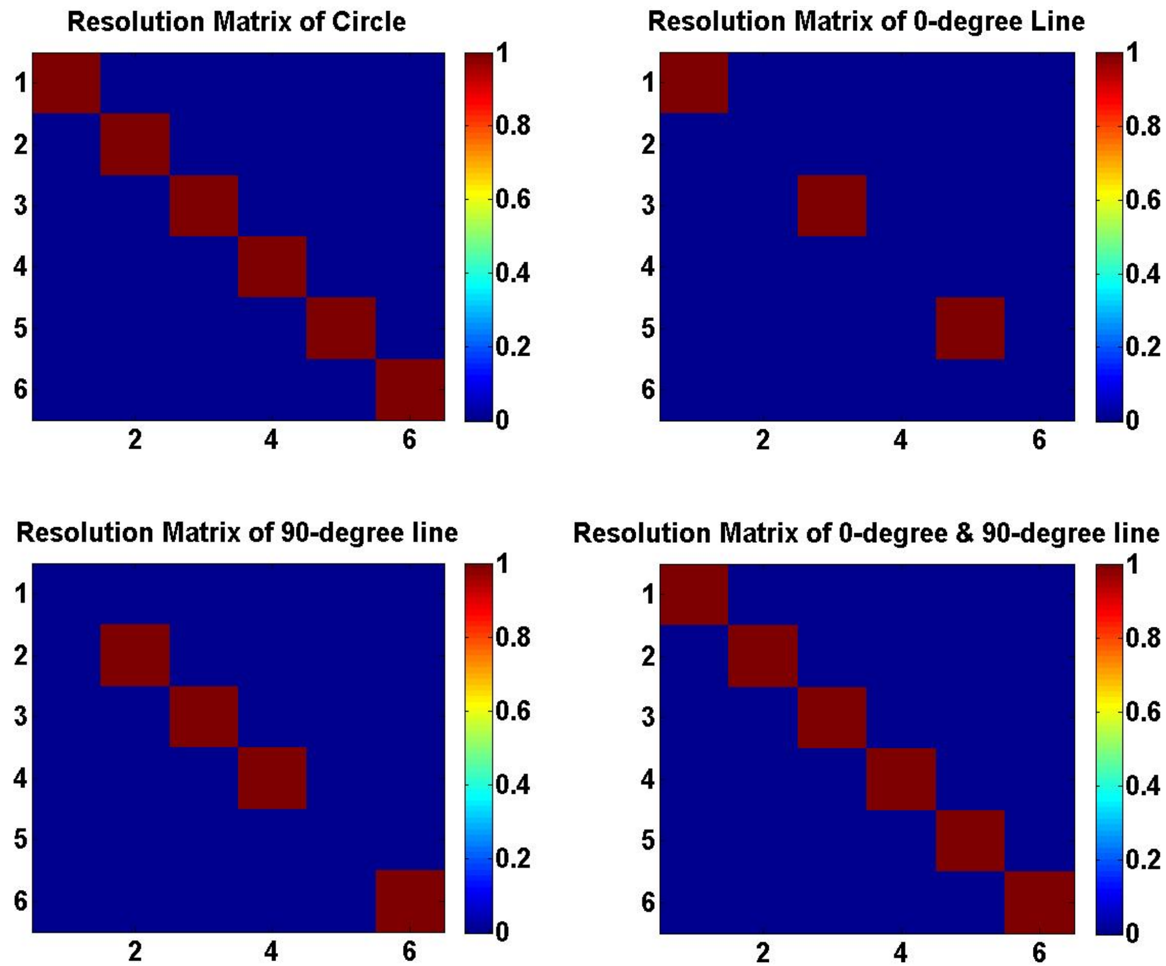

Body Wave Velocity (m/s)

CREWES

P	P	P	S	S	S
V_{11}	V_{22}	V_{33}	V_{23}	V_{13}	V_{12}
3644.1	2955.1	3333.7	1451.6	1562.5	1785.7

Measured **V_{33}= 3358.2 m/s**
Calculated **V_{33}=3333.7 m/s**
Err% = **0.73 %**

V_{11}	V_{22}	V_{33}	V_{23}	V_{13}	V_{12}
3640	2950	3500	1510	1530	1700

Faranak Mahmoudian

V_{11}	V_{22}	V_{33}	V_{23}	V_{13}	V_{12}
3576	2925	3365	1506	1602	1665

Scott P. Cheadle

PART 2: SOUTH KOMIE 3D DATA ANALYSIS

Horn River Basin

- **Location: Northeast BC & Southwest NT**

- **Area: 18,000 km²**
  Producing well: 200 (Feb 2014)

- **OGIP: 500 Tcf**

Compare to: Cordova: 200 Tcf;
Montney: 2000 Tcf

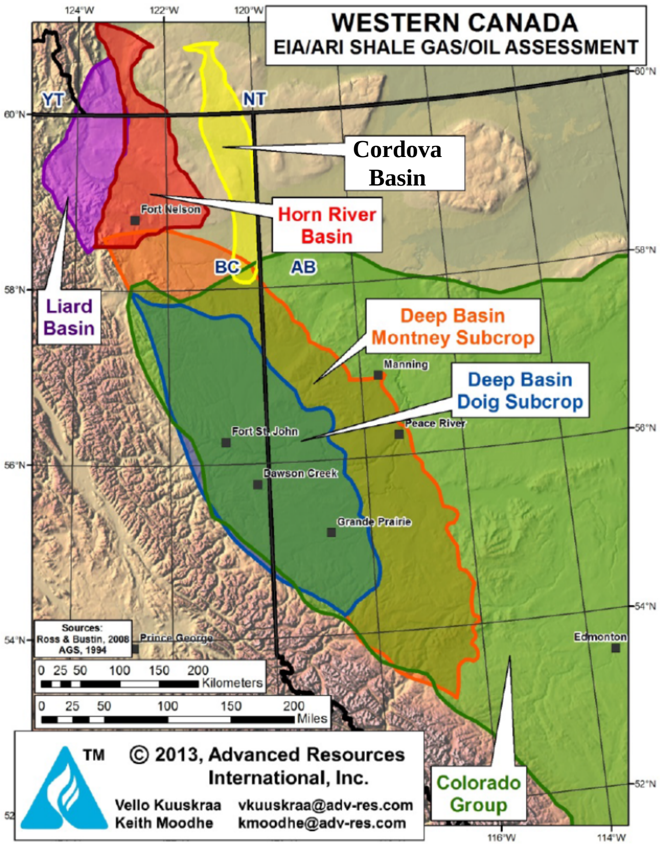

Stratigraphy

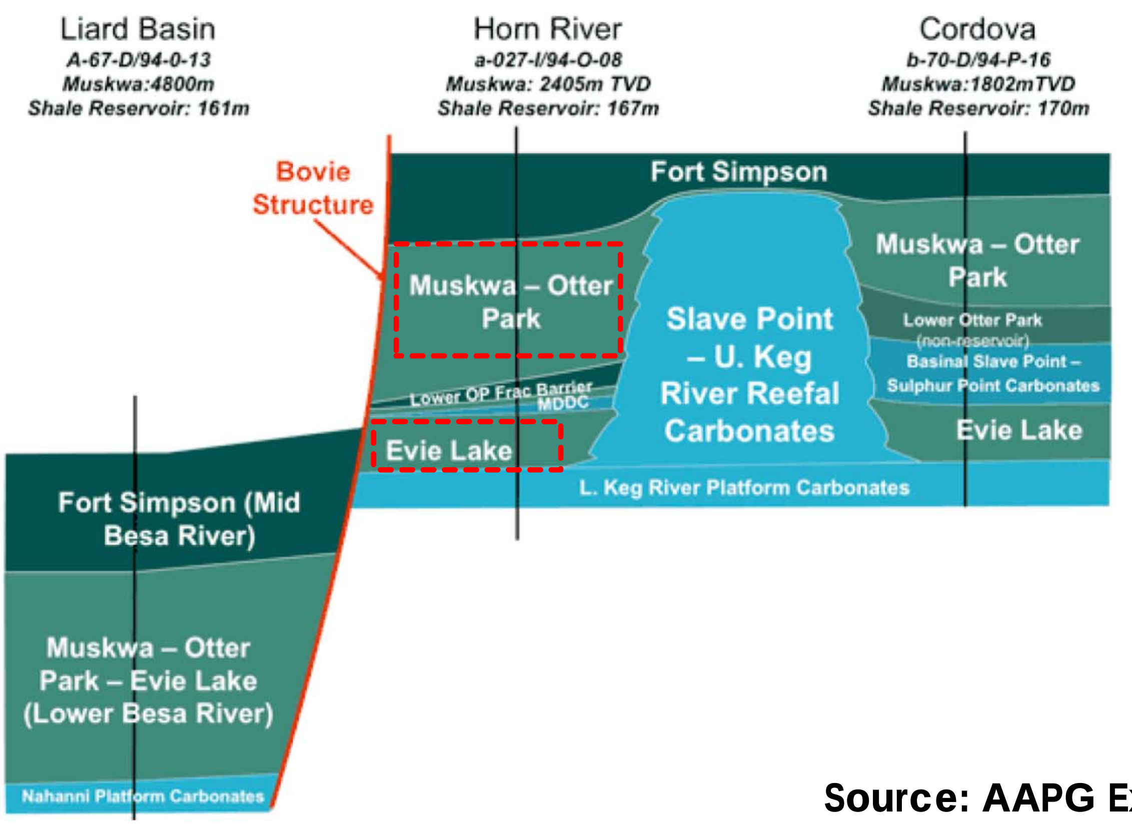

Source: AAPG Explorer, Horn River Basin Keeping Canada Hot

Data Acquisition

- Acquisition data: 12-29 March 2009
- Source: Dynamite (single hole)
  2 kg at 15 m depth
- Receiver: single 3-C
- Sample interval: 2 ms
- Source interval: 60 m Receiver interval: 60 m
- Source Line orientation: N-S
- Source Line spacing: 360 m
- Receiver line orientation: E-W
- Receiver line spacing: 240 m

Data processing

- Geometry
- Amplitude recovery
- Refraction Statics Correction
- Other statics
- Linear-noise attenuation
- Surface-consistent Decon
- Noise suppression
- NMO
- 3D COV Binning
- Migration Velocity Analysis
- 3D PSTM

Near-surface: 2nd refractor

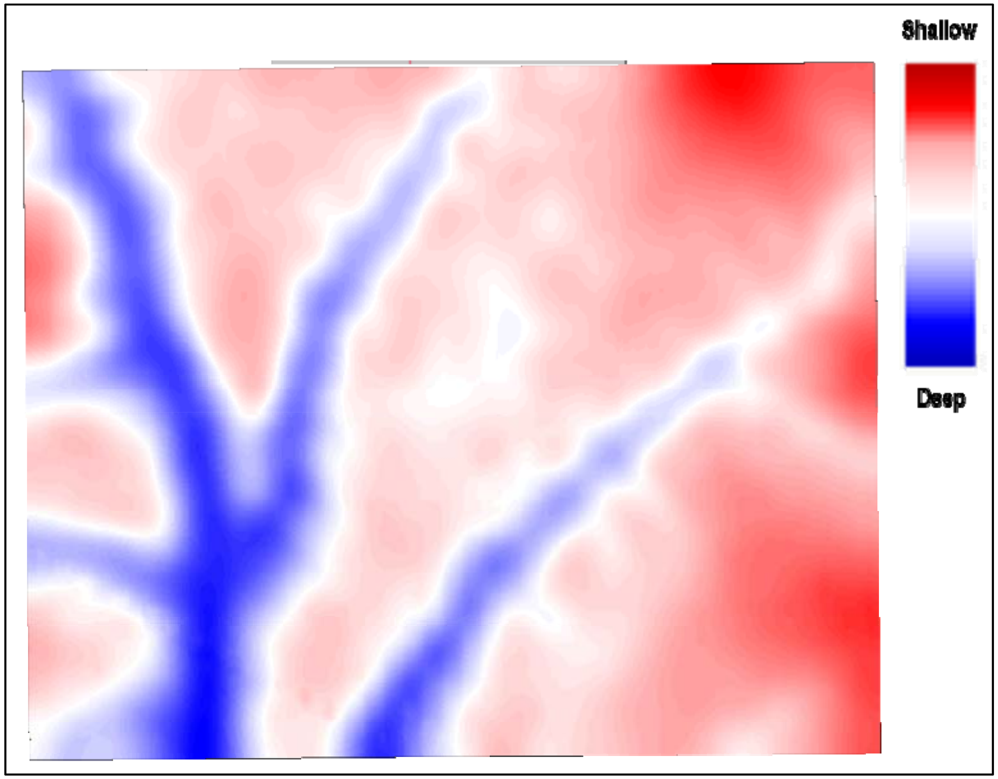

2nd refractor elevations:

A significant channel system within the near surface is observed.

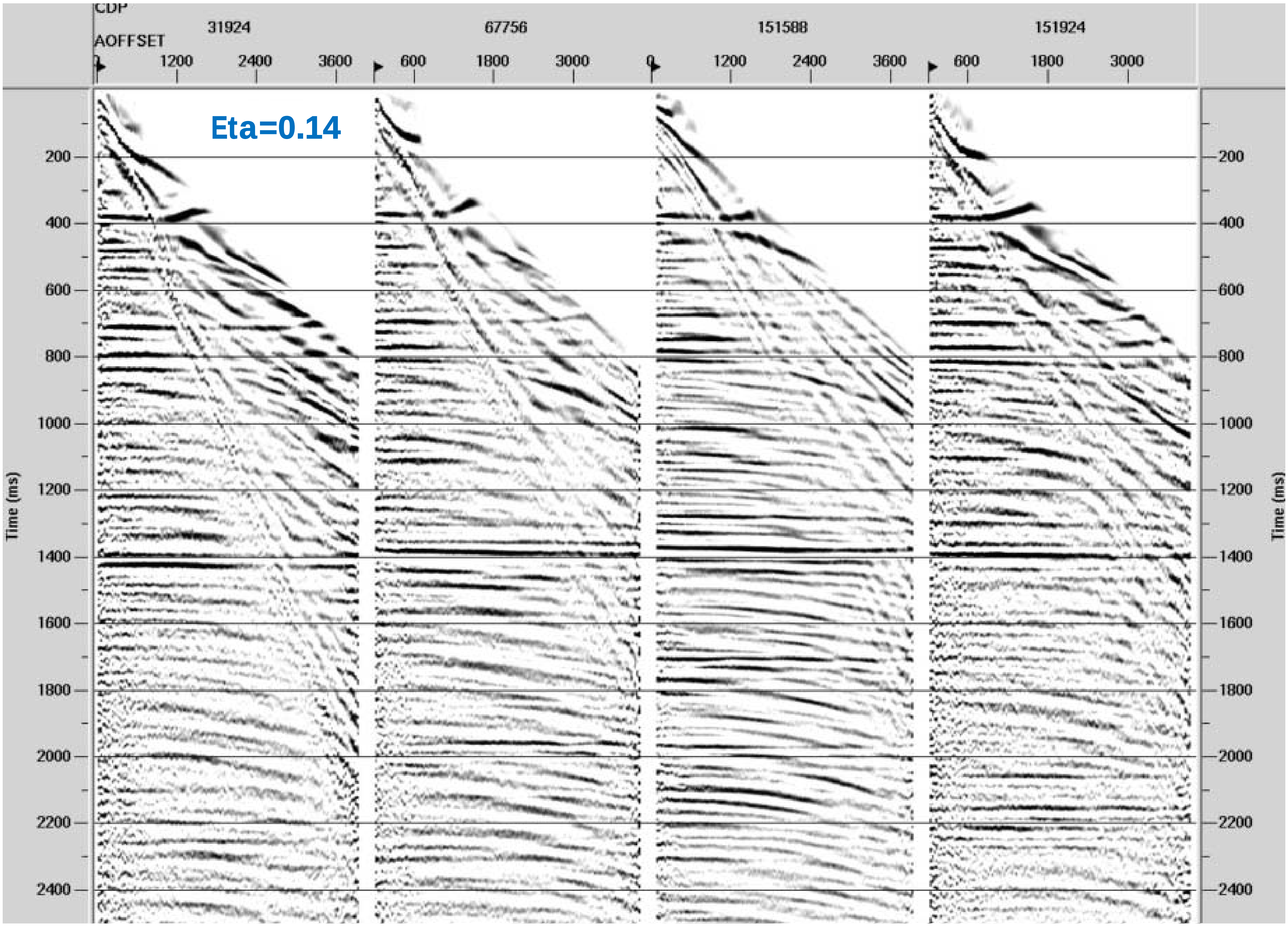

CDP
AOFFSET
31924
67756
151588
151924
0
1200
2400
3600
600
1800
3000
Eta=0.14
Time (ms)
200
400
600
800
1000
1200
1400
1600
1800
2000
2200
2400

PSTM Gathers

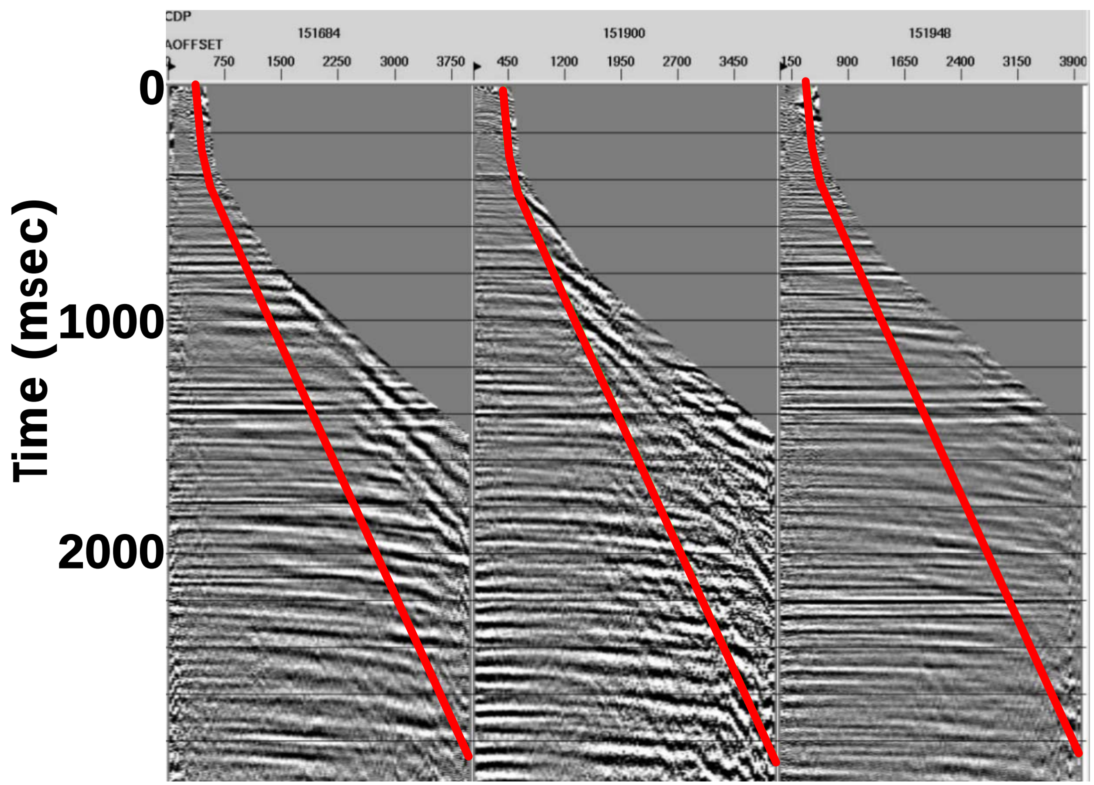

PSTM image gathers with an outer mute function indicated by green

PSTM Stack & Picked Horizons

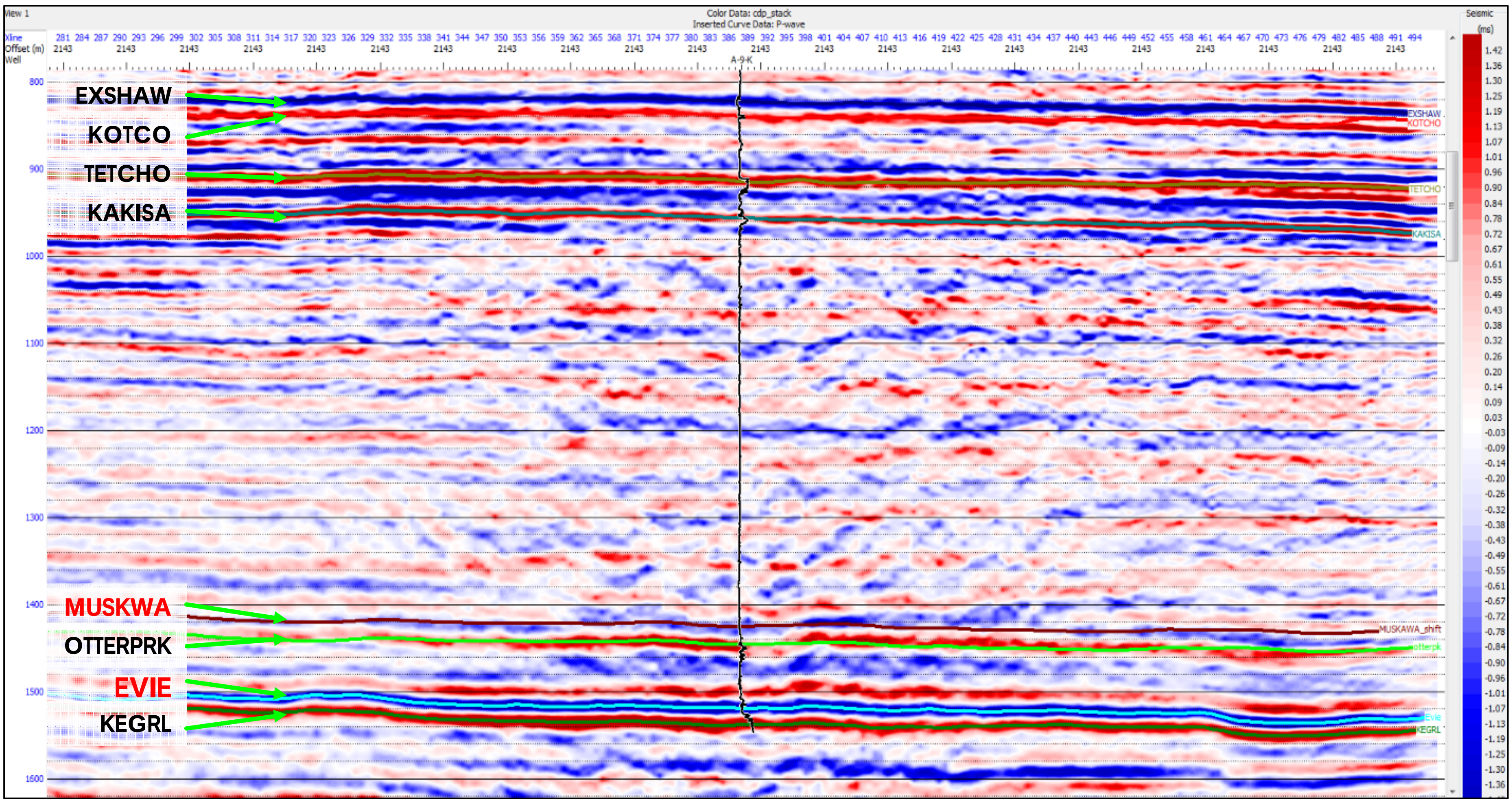

Well Log Correlation

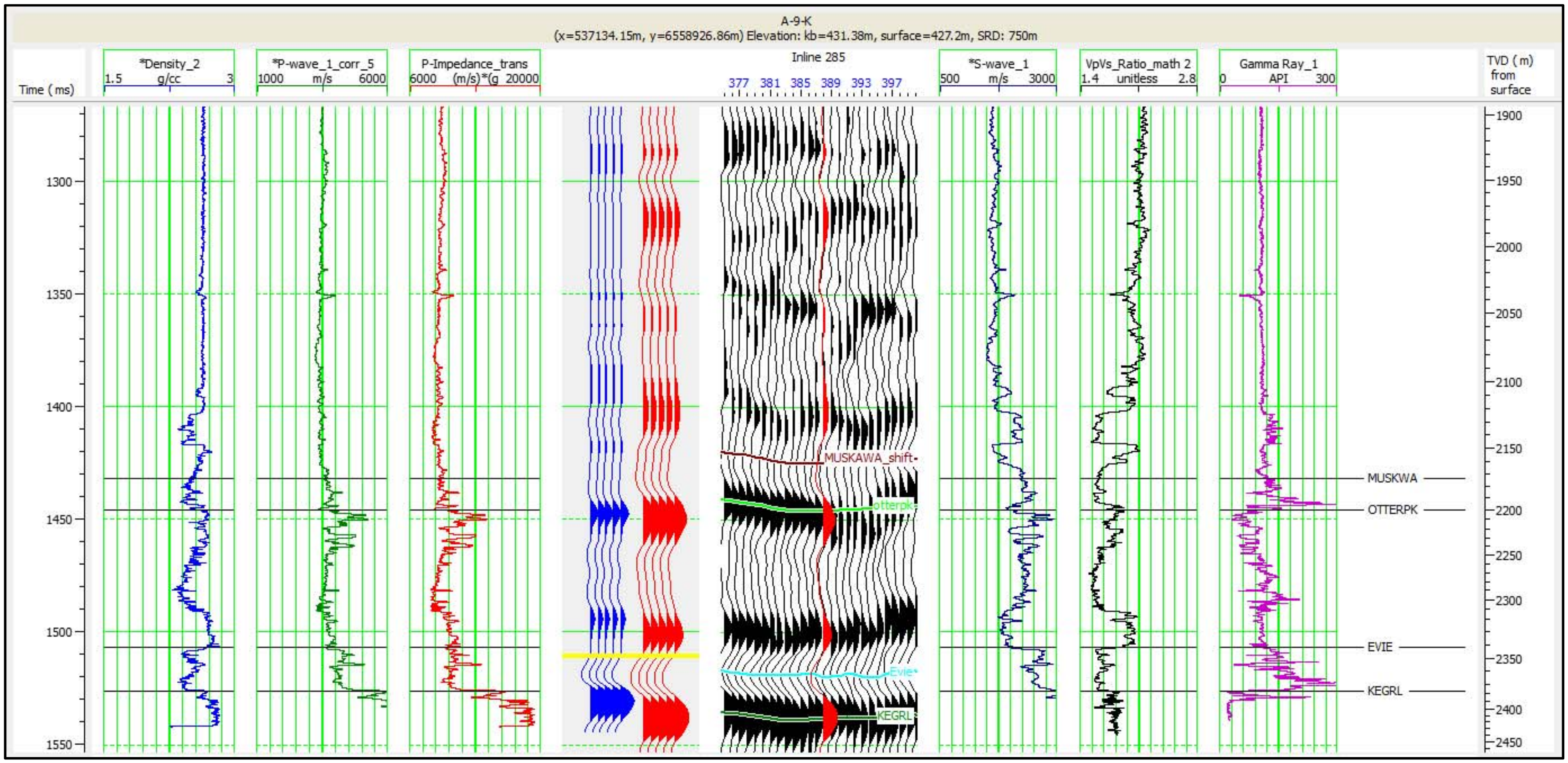

Target horizons:
Muskwa (left) & Evie (right)

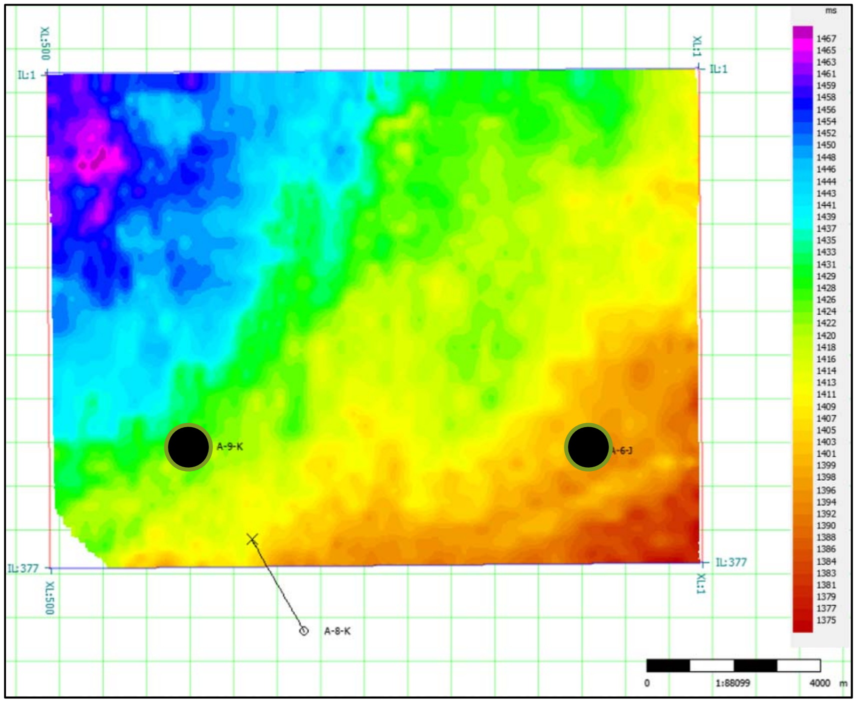

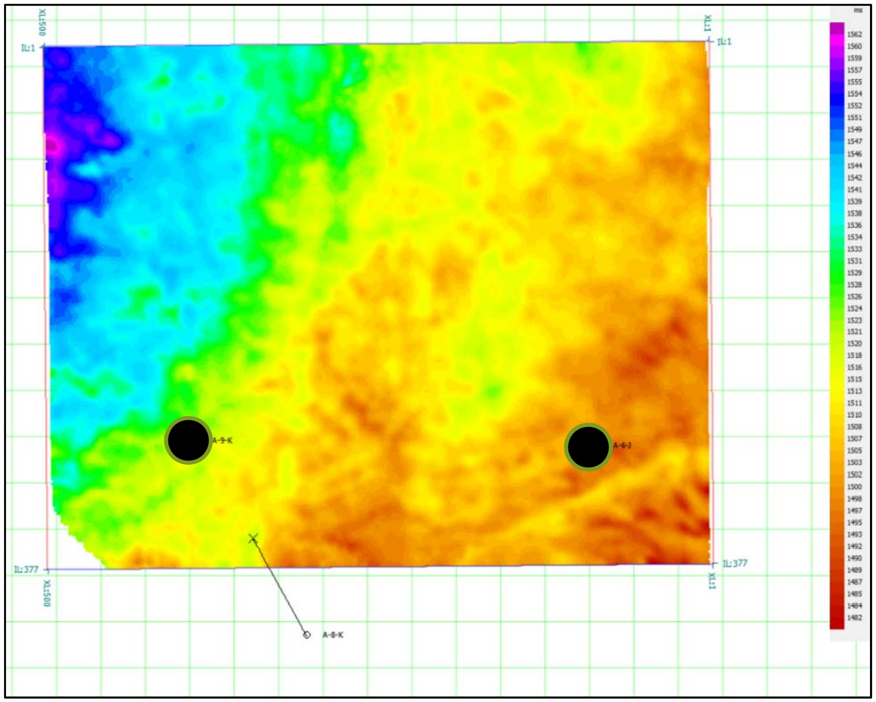

Post-stack Inversion

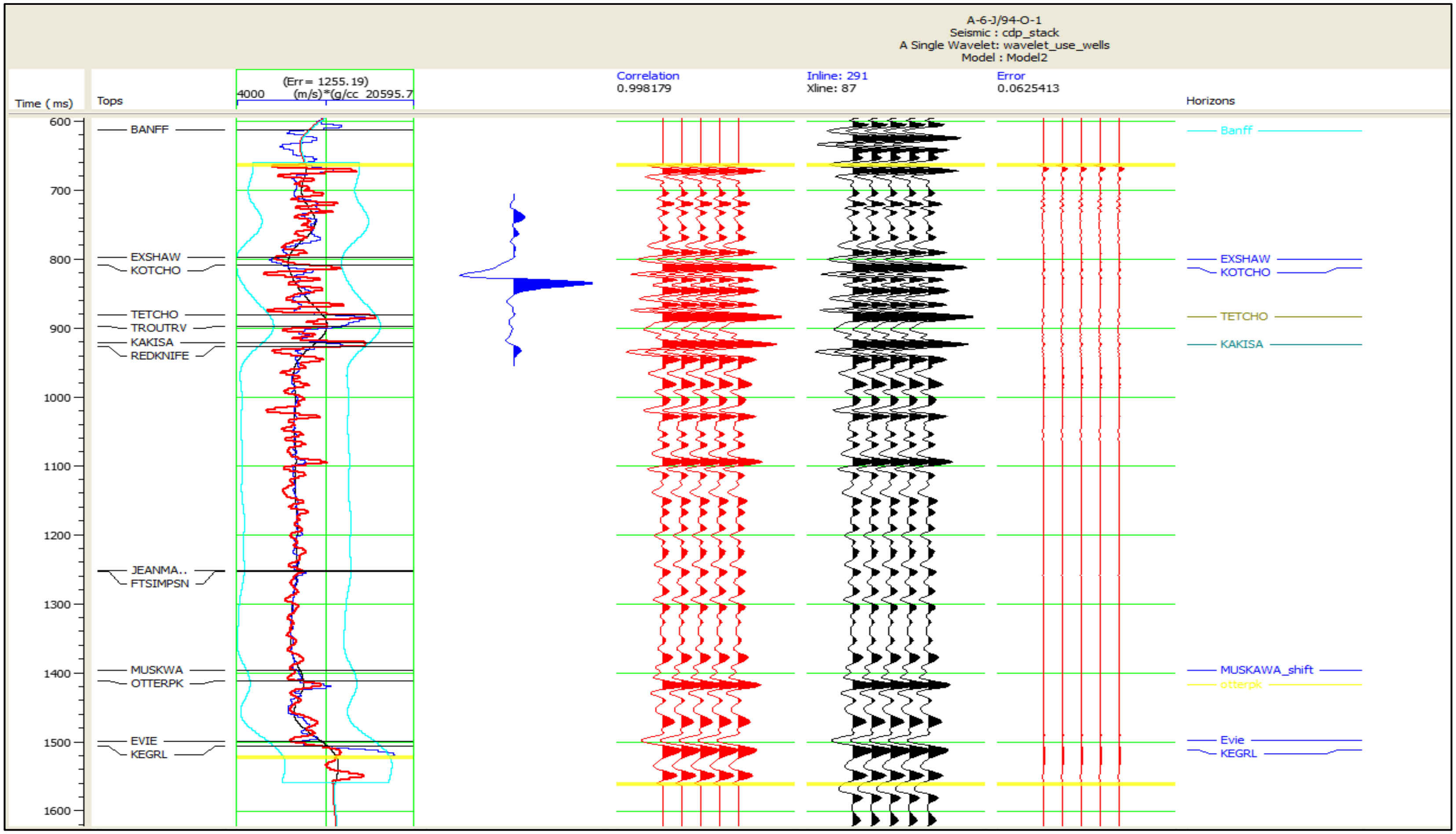

P-Impedance

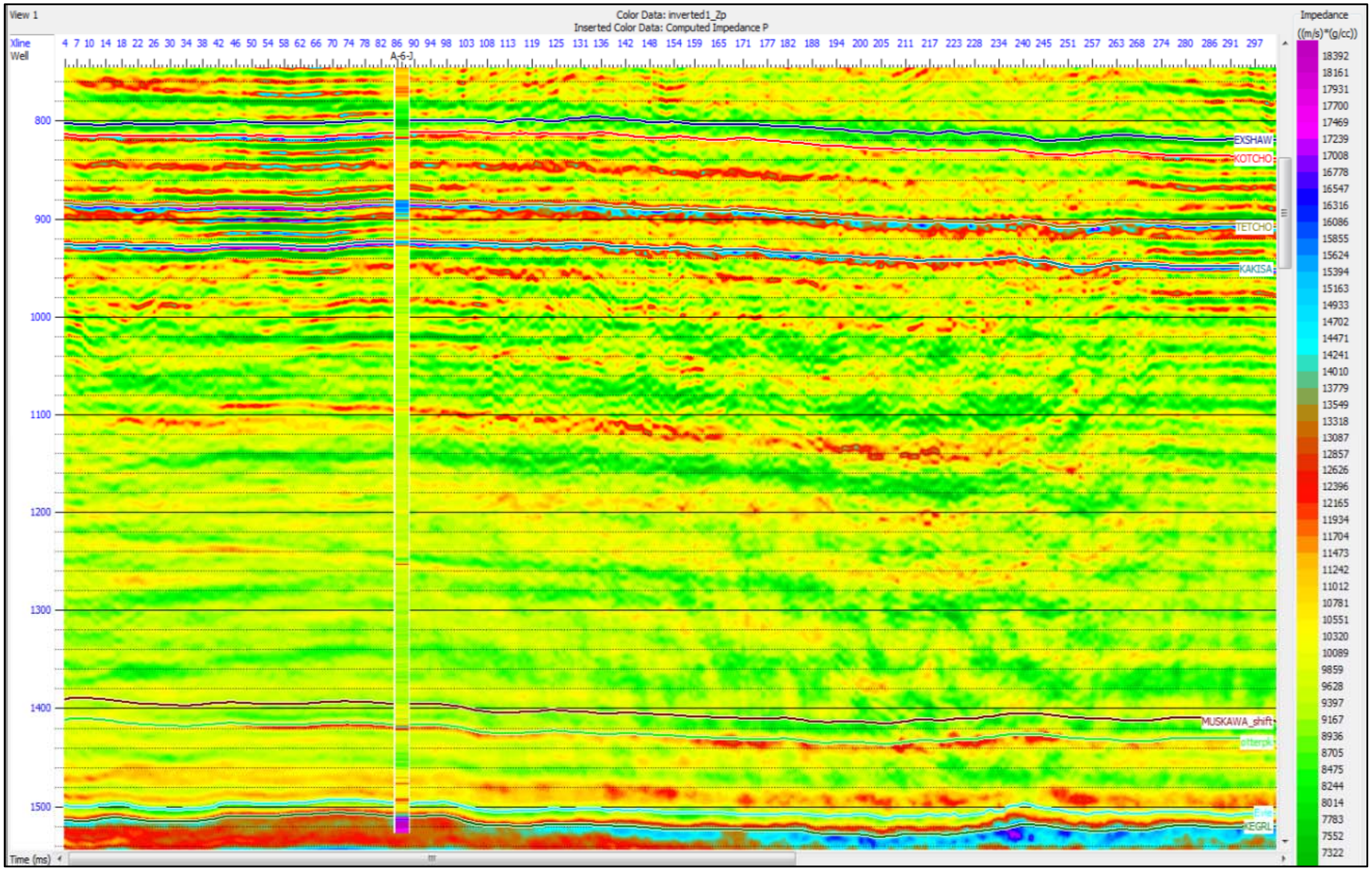

View 1
Color Data: inverted1_Zp
Inserted Color Data: Computed Impedance P
Xline
Well
4 7 10 14 18 22 26 30 34 38 42 46 50 54 58 62 66 70 74 78 82 86 90 94 98 103 108 113 119 125 131 136 142 148 154 159 165 171 177 182 188 194 200 205 211 217 223 228 234 240 245 251 257 263 268 274 280 286 291 297
A-6-J
800
900
1000
1100
1200
1300
1400
1500
Time (ms)
EXSHAW
KOTCHO
TETCHO
KAKISA
MUSKAWA_shift
KEGRL
Impedance
((m/s)*(g/cc))
18392
18161
17931
17700
17469
17239
17008
16778
16547
16316
16086
15855
15624
15394
15163
14933
14702
14471
14241
14010
13779
13549
13318
13087
12857
12626
12396
12165
11934
11704
11473
11242
11012
10781
10551
10320
10089
9859
9628
9397
9167
8936
8705
8475
8244
8014
7783
7552
7322

P-Impedance

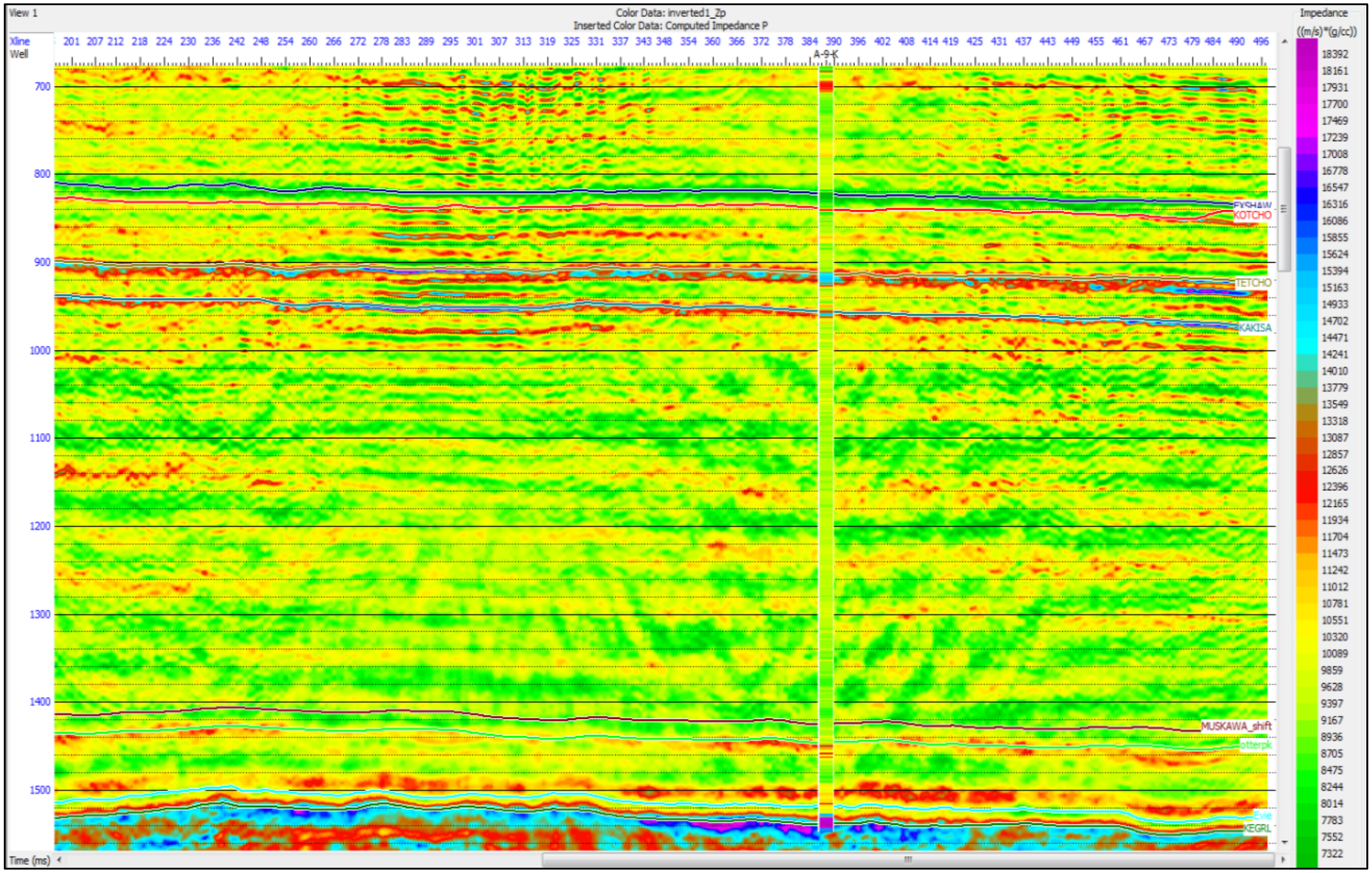

RMS amplitude at the Evie, sectored by S-R azimuth

Red arrows indicate azimuths. Black indicate lower amplitude values, or in another word lower impedance contrast. Therefore, it indicates the direction of fracture strike. Major directions are 0o (i.e. Well A-9) and 90o (i.e. Well A-6).

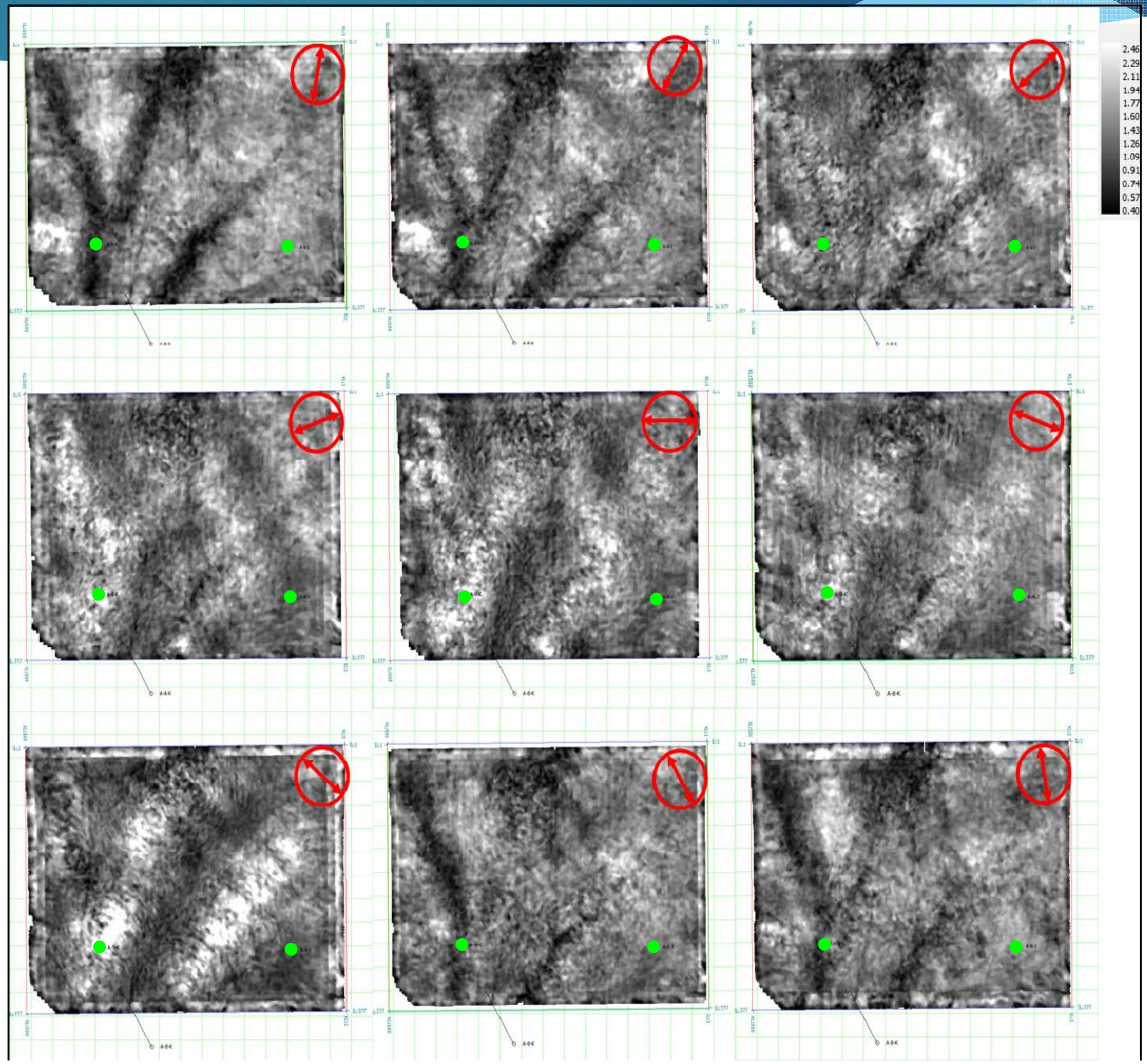

Instantaneous frequency at the Evie

Black Arrows indicate azimuth. Lower instantaneous frequencies see more fractures. Therefore, higher values indicate the fracture strike. Major direction are 90º

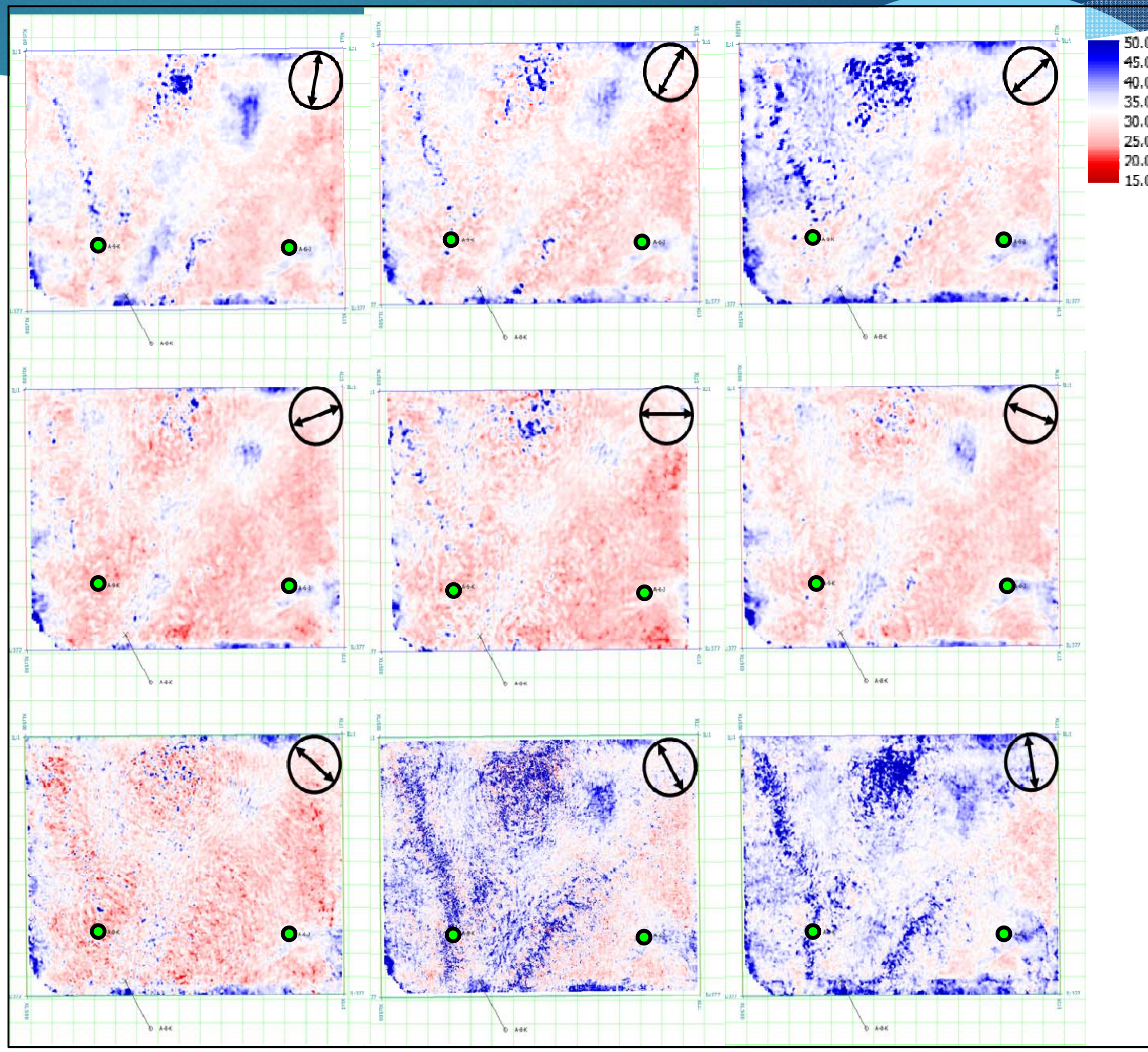

Curvature at the Evie

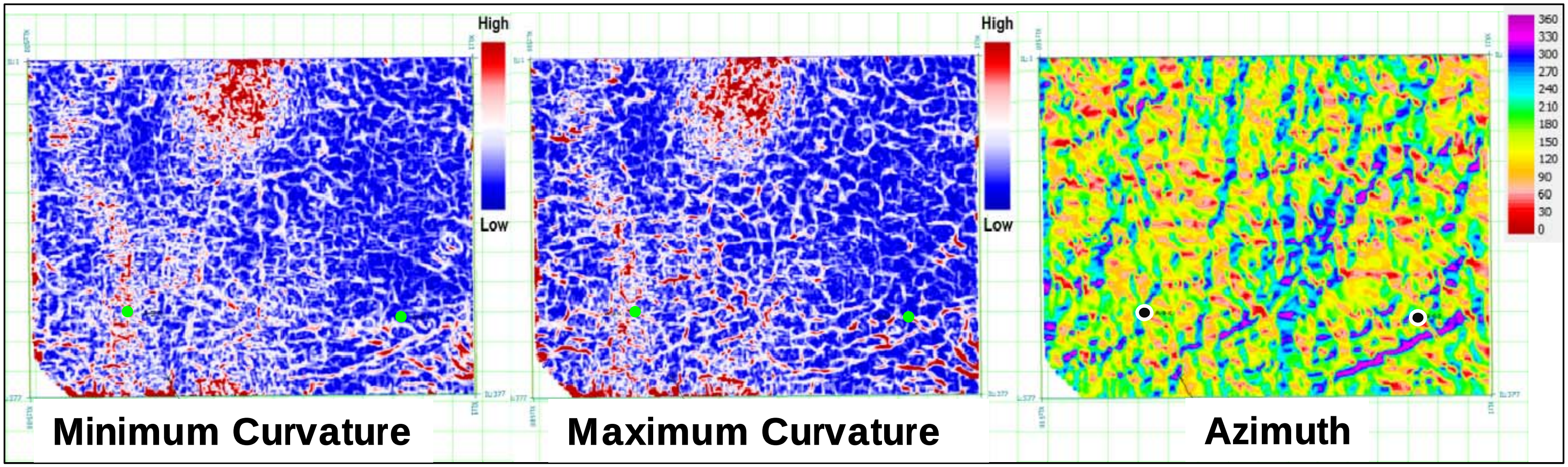

High curvature values indicate fractured zones. Azimuth map indicates that the major trends are about 0º and 40º.

CONCLUSIONS

Conclusions

- Stiffness coefficients matrix is calculated from physical modeling data using group velocity measurements form 3 common-receiver gathers
- Post-stack P-impedance inversion is utilized to indicate sweet spots
- post-stack amplitude, instantaneous frequency, and curvature attributes are utilized for identifying fracture direction and intensity

CREWES

Acknowledgments

- CREWES sponsors for their support
- NSERC for the grant CRDPJ 379744-08
- Seitel and Arcis for permission to use the data and publish the results
- Geophysical Sensor for time processing of the data
- CGGVeritas for the use of Hampson-Russell software
- Dr. Don Lawton, Dr. Faranak Mahmoudian, Nassir Saied, Jesse Kolb, Dr. Helen Isaac, and Dr. Pat Daley
- Saudi Aramco for PhD sponsorship of the first author

UNIVERSITY OF CALGARY

CREWES

Thank you

Khaled Al Dulaijan
kaldulai@ucalgary.ca

NSERC
CRSNG

AVO Analysis: Synthetic

AVO modelling: synthetic angle gather (left), amplitude curves (middle), and intercept vs. gradient plot (right).

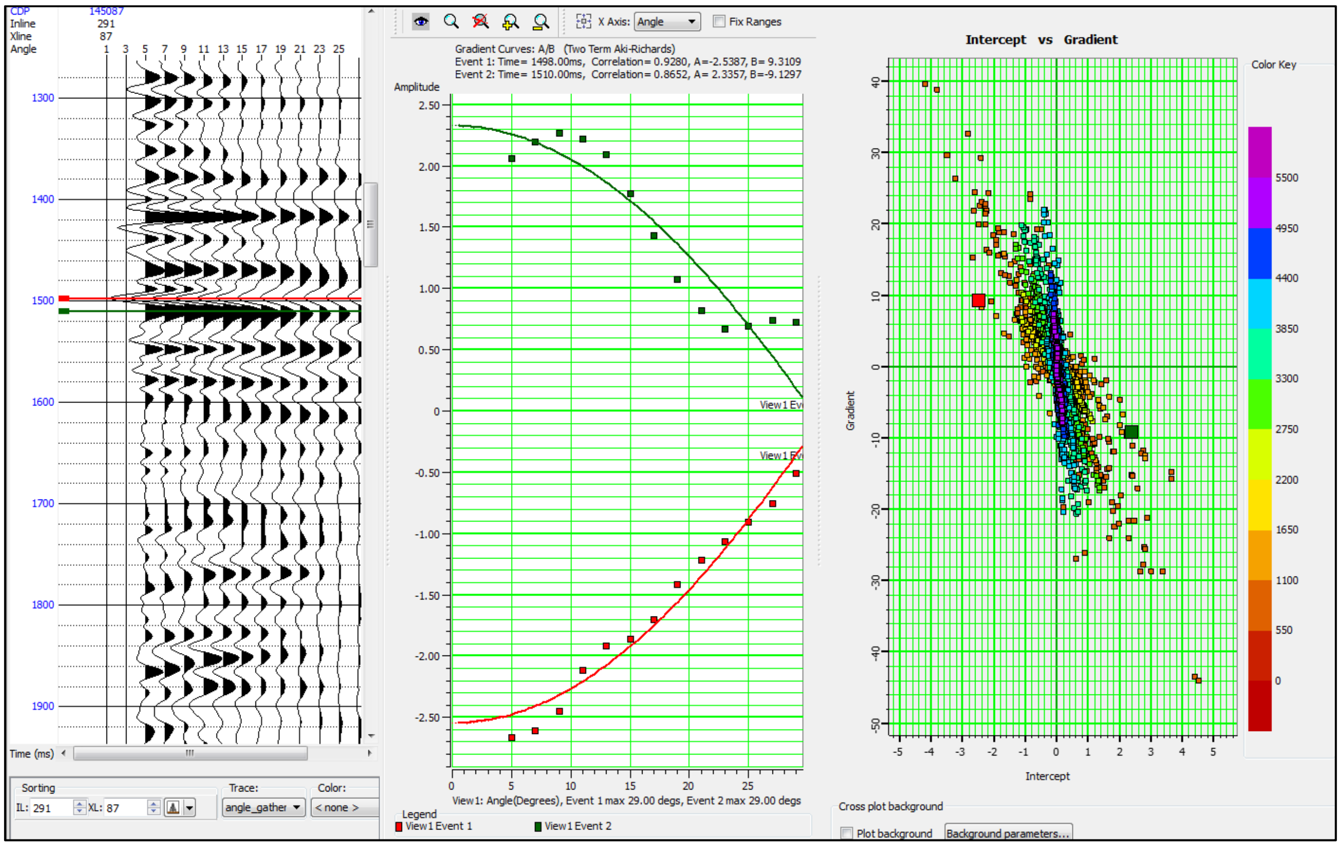

Super gathers

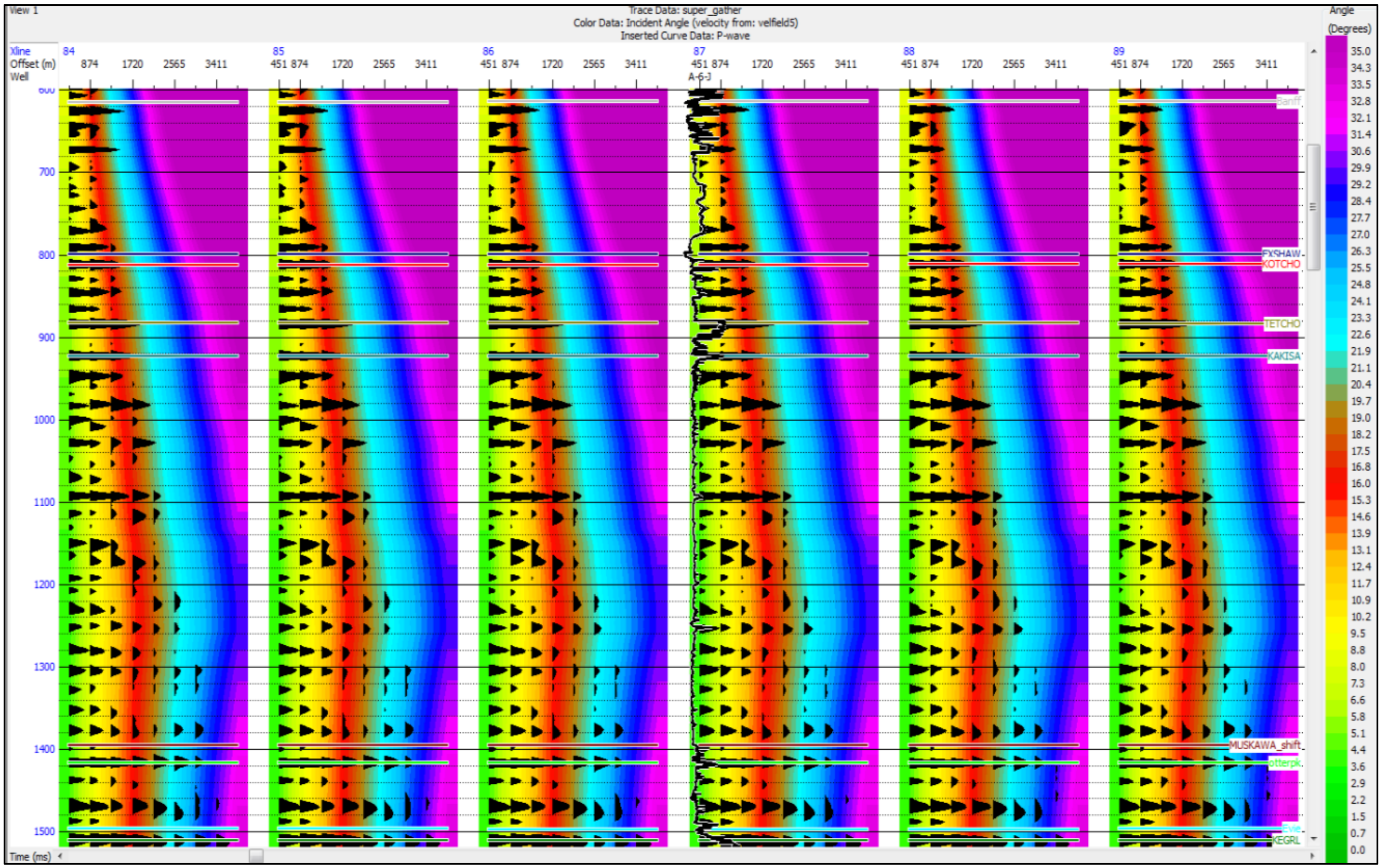

Angle gathers & Amplitude vs Angle

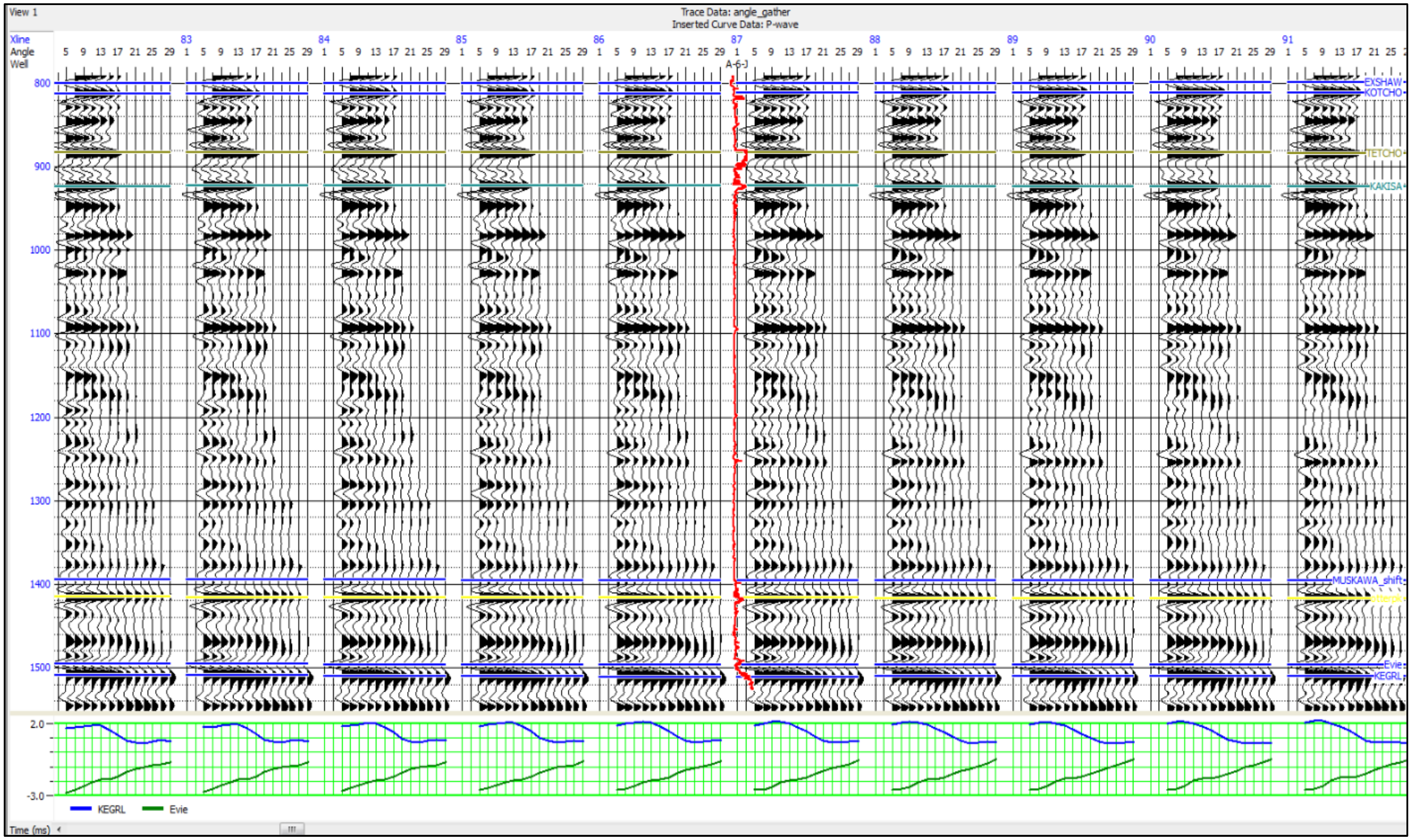

AVO

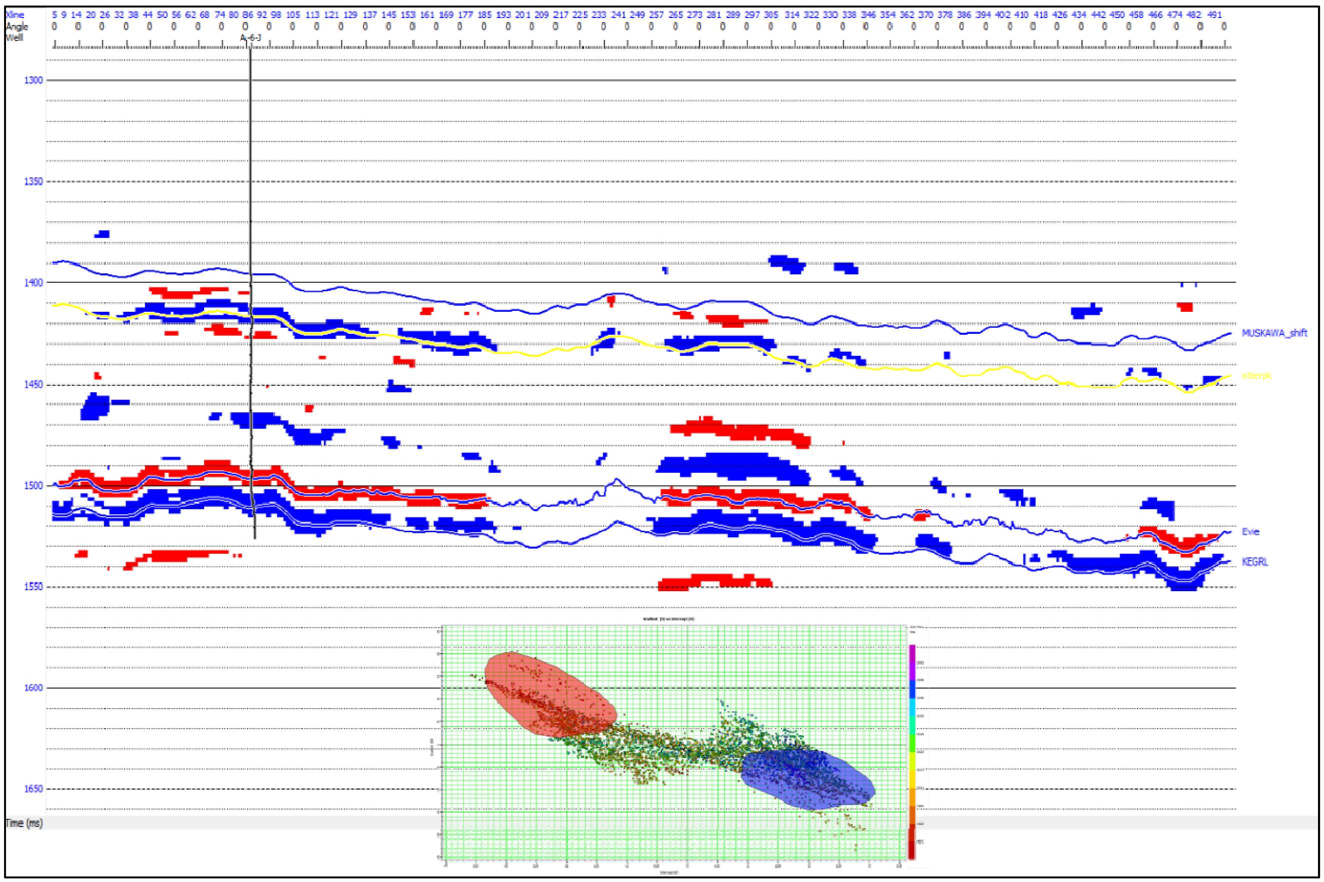

class IV reservoir. Red is top & blue is bottom of the reservoir.